This document is confidential and is proprietary to the American Chemical Society and its authors. Do not copy or disclose without written permission. If you have received this item in error, notify the sender and delete all copies.

Temperature-responsive polymersomes of poly(3-methy-N-vinylcaprolactam)-block-(poly(N-vinylpyrrolidone) to decrease doxorubicin-induced cardiotoxicity

Journal:	*Biomacromolecules*
Manuscript ID	bm-2019-01026g.R1
Manuscript Type:	Article
Date Submitted by the Author:	06-Sep-2019
Complete List of Authors:	Kozlovskaya, Veronika; University of Alabama at Birmingham, Chemistry Liu, Fei; University of Alabama at Birmingham, Chemistry Yang, Yiming; University of Alabama at Birmingham, Chemistry Ingle, Kevin; University of Alabama at Birmingham, Medicine Qian, Shuo; Oak Ridge National Laboratory, Center for Structural Molecular Biology, Neutron Scattering Sciences Division and Chemical Sciences Division Halade, Ganesh; University of Alabama at Birmingham, Medicine Urban, Volker; Oak Ridge National Laboratory, Biology and Soft Matter Division Kharlampieva, Eugenia; University of Alabama at Birmingham, Chemistry

SCHOLARONE™
Manuscripts

Temperature-responsive polymersomes of poly(3-methy-N-vinylcaprolactam)-block-(poly(N-vinylpyrrolidone) to decrease doxorubicin-induced cardiotoxicity

Veronika Kozlovskaya,[1] Fei Liu,[1] Yiming Yang,[1] Kevin Ingle,[2] Shuo Qian,[3] Ganesh V. Halade,[2] Volker S. Urban,[3] Eugenia Kharlampieva*,[1,4]

[1]Department of Chemistry, [2]Division of Cardiovascular Disease, Department of Medicine, University of Alabama at Birmingham, Birmingham, Alabama 35294, United States

[3] Neutron Scattering Division, Neutron Sciences Directorate, Oak Ridge National Laboratory, Oak Ridge, Tennessee 37831, United States

[4]Center for Nanoscale Materials and Biointegration, University of Alabama at Birmingham, Birmingham, Alabama 35294, United States

KEYWORDS:
poly(N-vinylcaprolactam), poly(N-vinylpyrrolidone), poly(N-vinyl-3-methylcaprolactam), polymersomes, liposomes, doxorubicin, cardiac toxicity

ABSTRACT

Despite being one of the most potent chemotherapeutics, doxorubicin (DOX) facilitates cardiac toxicity by irreversibly damaging the cardiac muscle as well as severely dysregulating the immune system and impairing the resolution of cardiac inflammation. Herein, we report synthesis and aqueous self-assembly of nanosized polymersomes from temperature-responsive poly(3-methyl-N-vinylcaprolactam)-*block*-poly(N-vinylpyrrolidone) (PMVC-PVPON) diblock copolymers and demonstrate their potential to minimize DOX cardiotoxicity compared to liposomal DOX. RAFT polymerization of vinylpyrrolidone and 3-methyl-N-vinylcaprolactam, which are structurally similar monomers but have drastically different hydrophobicity, allows decreasing the cloud point

of $PMVC_m$-$PVPON_n$ copolymers below 20 °C. The lower critical solution temperature (LCST) of the $PMVC_{58}$-$PVPON_n$ copolymer was varied from 19.2 to 18.6, and to 15.2 °C by decreasing the length of the hydrophilic $PVPON_n$ block from n = 98 to n = 65, and to n = 20. The copolymers assembled into stable vesicles at room temperature when PVPON polymerization degree was 65 and 98. Anticancer drug DOX was entrapped with high efficiency into the aqueous $PMVC_{58}$-$PVPON_{65}$ polymersomal core surrounded with the hydrophobic temperature-sensitive PMVC shell and the hydrophilic PVPON corona. Unlike many liposomal, micellar or synthetic drug delivery systems, these polymersomes exhibit an exceptionally high loading capacity of DOX (49%) and encapsulation efficiency (95%) due to spontaneous loading of the drug at room temperature from aqueous DOX solution. We also show that C57BL/6J mice injected with the lethal dose of DOX at 15 mg kg^{-1} did not survive the 14-day treatment, resulting in 100% mortality. The DOX-loaded $PMVC_{58}$-$PVPON_{65}$ polymersomes did not cause any mortality in mice indicating that they can be used for successful DOX encapsulation. The gravimetric analyses of the animal organs from mice treated with liposome-encapsulated DOX (Lipo-DOX) and $PMVC_{58}$-$PVPON_{65}$ polymersomes (Poly-DOX) revealed that the Lipo-DOX injection caused some toxicity manifesting as decreased body weight compared to Poly-DOX and saline control. Masses of the left ventricle of the heart, lung, and spleen were reduced in the Lipo-DOX treated mice compared to the non-toxic saline control, while no significant decrease of those masses was observed for the Poly-DOX treated mice. Our results provide evidence for superior stability of synthetic polymersomes *in vivo* and show a promise for the development of next-generation drug carriers with minimal side effects.

INTRODUCTION

Doxorubicin (DOX) is a widely used FDA-approved therapeutic for cancer treatment. However, it triggers the development of progressive heart failure.[1,2] DOX can facilitate cardiac toxicity by irreversibly damaging the cardiac muscle as well as severely dysregulating the immune system and impairing the resolution of cardiac inflammation.[3,4] Although the severity of DOX side effects is considered to be dose- and treatment-time dependent,[5] noninvasive imaging approaches of heart tissues such as magnetic resonance imaging and echocardiography can reveal the early subclinical cardiotoxicity[6,7] manifesting as acute cardiac dysfunctions including acute ischemia and infarction,[8] and abnormal heart muscle thickening or shortening.[9,10] Chronic cardiotoxicity can manifest as diastolic or systolic dysfunction and result in heart failure and arrhythmias long after the chemotherapy treatment.[11]

To mitigate acute or delayed DOX toxicity, a variety of drug delivery systems have been developed and investigated including liposomes,[11,12] polymeric nanoparticles and conjugates,[13,14] and micelles.[15,16,17] Unlike rigid nanoparticles and drug-polymer conjugates that suffer from rapid blood clearance,[18] tissue toxicity,[19] and activation of complex immune response, liposomes assembled from synthetic lipid molecules can have much higher drug loading capacity shielding drugs inside the hollow cavity from immunologic clearance.[20,21] However, lower chemical and physical stability of liposomes can lead to their instability in the blood.[22,23] Liposomes have been shown to undergo significant drug leakage while in circulation and rapid recognition by the reticuloendothelial system (RES) resulting in short half-lives.[11,24] Incorporation of poly(ethylene glycol) (PEG)-lipids within the liposomal bilayer has been shown to increase their blood circulation time due to formation of the highly hydrophilic steric layer of PEG which could drastically reduce their macrophage recognition and RES uptake.[25,26]

In this respect, polymer nanostructures assembled from amphiphilic block copolymers including micelles, nanoparticles, nanovesicles and multicompartment nanocarriers have been intensively studied for anticancer drug delivery since their small size (≤ 200 nm) allows accumulation in tumors due to the enhanced permeability and retention arising from cancerous vasculature.[20,21,27, 28,29,30] AB type block copolymers with hydrophilic (A block) and hydrophobic (B-block) regions can self-assemble into polymer vesicles (polymersomes) and mimic natural lipid bilayers within a cell membrane.[31-35] In contrast to liposome-based carriers which exhibit short half-lives, low oxidation stability, and may suffer from leakage and fusion,[36] the composition, structure, and physicochemical properties of polymeric vesicles can be easily controlled by the high diversity of block copolymer structures.[37 - 41] Regardless of the assembly method, polymersomes demonstrate efficient drug entrapment, long shelf life, and can be imparted with controllable stimuli-triggered release of payload including pH, temperature, and degradable linkages.[42,43,44,45]

For self-assembly into polymersomes stable at room temperature, amphiphilic diblock copolymers are usually dissolved in organic solvents followed by mixing with water to initiate the aggregation of the hydrophobic blocks into a bilayer structure.[33] The use of organic media might not be always compatible with the encapsulation of proteins, therapeutic peptides or and nucleic acids and may require laborious multistep synthesis, self-assembly and purification efforts.[46,47] We have recently developed double hydrophilic block copolymers based on temperature-responsive poly(N-vinylcaprolactam) (PVCL) using RAFT polymerization, which could self-assemble into polymeric vehicles upon temperature increase due to the coil-to-globule transition of the PVCL chains at lower critical solution temperature of the PVCL-based blocks.[48,49] Unlike the sharp volume-phase transition of temperature-sensitive poly(N-isopropylacrylamide),[50] PVCL

exhibits a continuous coil-to-globule phase transition from 36 to 50 °C, depending on the polymer molar mass and concentration,[51] allowing for controlling the lower critical solution temperature (LCST) of PVCL via changes in the polymer chain length.[52, 53] The PVCL-*b*-poly(N-vinylpyrrolidone) (PVPON) block copolymer vehicles have been demonstrated to easily adjust their size depending on the length of the hydrophilic PVPON block.[48] However, due to the LCST of PVCL being higher than 36 °C, the self-assembled structures from PVCL-*b*-PVPON block copolymers were not stable at the physiological temperature[48, 54] but their polymersomal morphology could be stabilized through hydrogen-bonded interactions of the shell corona with polyphenol performed at 40-50 °C.[55]

By copolymerizing N-vinylcaprolactam with hydrophobic monomers of vinyl acetate and N-methyl-N-vinylacetamide, the hydrophilicity of PVCL-based statistical copolymers could be lowered significantly to exhibit the cloud points at 20 °C, however, the LCSTs of the corresponding PVCL block copolymers could not be decreased below 40 °C.[56] In our previous study, we showed that by copolymerizing structurally-similar monomers of N-vinylcaprolactam and 3-methyl-N-vinylcaprolactam, the LCST of the statistical copolymer can be controlled in the range of physiological temperatures from 19 to 42 °C.[49] The obtained poly(methyl-vinylcaprolactam-co-vinylcaprolactam)-*b*-poly(vinylcaprolactam-co-vinylpyrrolidone) diblock copolymers assembled into micelles at T = 25 °C and release DOX due to temperature-induced micelle aggregation at 42 °C.[49] However, those random copolymers were not able to produce vesicular structures.

In the current study, we have developed thermosensitive polymersomes undergoing self-assembly in water at decreased temperatures (T < 20 °C) using newly synthesized amphiphilic diblock copolymers of poly(3-methyl-N-vinylcaprolactam)$_{58}$-*b*-PVPON$_n$ (PMVC-PVPON) with n

= 20, 65, 98. The block-copolymers with n = 65 and 98 are capable of self-assembly into polymersomes due to their low LCST varied from 15 to 19 °C, which is controlled via a hydrophobic modification of the N-vinylcaprolactam monomer and varying the ratio of the PMVC and PVPON blocks. We also explore the loading and release of the $PMVC_{58}$-$PVPON_{65}$ polymersomes with DOX and its stability in serum. Finally, we investigate the cardiotoxicity of the DOX-loaded $PMVC_{58}$-$PVPON_{65}$ polymersomes in comparison to DOX-loaded liposomes injected in mice using *in vivo* transthoracic electrocardiography of mice followed by gravimetric and necropsy analysis. We compare cardiotoxicities of the polymersomes and liposomes loaded with DOX at high (15 mg kg^{-1}; survival 0%) dose after 14 days, and demonstrate their effects on the heart. Our results provide the evidence for superior stability of synthetic polymersomes *in vivo*, and with further development into a degradable vehicle by introducing a degradable linkage between polymer blocks may show potential to be further developed into a clinically relevant therapeutic carriers expanding the next generation of advanced therapeutic carriers with minimal side effects.

EXPERIMENTAL SECTION

Materials. 2,2'-Azobis(2-methylpropionitrile) (AIBN) was purchased from Sigma-Aldrich and recrystallized from methanol before use. N-vinylcaprolactam (VCL) and N-vinylpyrrolidone (VPON) were purchased from Sigma-Aldrich and purified at low pressure before polymerization. 1,4-Dioxane, tetrahydrofuran, and diisopropylamine were from Sigma-Aldrich and were freshly distilled before use. Hexane, methyl iodide, butyl lithium, sodium, O-ethyl xanthic acid potassium, methanol were purchased from Fisher and used as received. Egg phosphatidylcholine (EPC) and (DSPE-PEG (2000)) (1,2- distearoyl-sn-glycero-3-phosphoethanolamine (polyethylene glycol)-2000) were obtained from Avanti Polar Lipids (Alabaster, AL, USA). Doxorubicin hydrochloride

(DOX) was purchased from LC Laboratories. Linear polystyrene standards for gel permeation chromatography (GPC) analysis were purchased from PSS USA Inc. Ultrapure deionized water with the resistivity of 18.2 Ω cm (Evoqua) was used for aqueous solutions.

Synthesis of 3-Methyl-N-vinylcaprolactam (MVC). In a dried Schlenk flask, diisopropylamine (17.7 mL, 126 mmol) and THF (170 mL) were mixed. The Schlenk flask was immersed in a dry ice/acetone bath (-78°C), and n-BuLi (50 mL, 2.5 M in hexane, 126 mmol) was then added dropwise into the solution within 10 min. The mixture was warmed to 0 °C in ice/water bath under stirring for 10 min and then was cooled back to -78 °C. N-vinylcaprolactam monomer (15 g, 108 mmol) was then slowly added into the solution within 5 min, and the mixture was kept at -78 °C for 1 h. Finally, methyl iodide (108 mmol) was added into the mixture, and the solution was slowly warmed to room temperature and stirred overnight. The [MVC]/[methyl iodide] ratio was kept at 1/1. The reaction was quenched by adding deionized (DI) water (200 mL). The organic phase was separated, and the aqueous layer was extracted three times with ethyl acetate (50 mL). The organic phases were combined, dried with Na_2SO_4, and concentrated by rotary evaporation. The raw product was purified using a silica column with ethyl acetate/petroleum ether (1:20 v/v) as eluent, yielding 3-methyl-N-vinylcaprolactam as colorless oil (yield: 13 g, 79%).

RAFT Synthesis of PMVC macroinitiator and PMVC-PVPON diblock copolymers. RAFT chain transfer agent (CTA) was prepared by drop-wise adding O-ethyl xanthic acid potassium (5.6 g, 35 mmol,) to methyl-2-bromopropionate (5 g, 30 mmol,) in methanol on ice bath. After 12-h reaction, the product was extracted with hexane/ethyl ether mixture (200 mL, 1:1, v/v) followed by drying on a rotovap. MVC monomer (6 g, 38 mmol), AIBN (5 mg, 0.03 mmol), freshly distilled 1,4-dioxane (2 mL) were mixed with the CTA (15 mg, 0.07 mmol) in a Schlenk flask ($[M]_0$/[CTA] ratio = 540/1 and the [CTA]/[I] ratio = 2.3/1) followed by three cycles of freeze-pump-thaw under

argon. The mixed solution was heated for 6 hours at 60 °C and the polymerization was quenched on a dry ice bath. The product (yield: 4.5 g, 75%) was purified by precipitation in hexane and characterized with nuclear magnetic resonance (^{1}H-NMR) and gel-permeation chromatography (GPC). ^{1}H NMR spectra of diblock copolymers were collected using Bruker 400 MHz NMR spectrometer. The diblock copolymer solutions were prepared in $CDCl_3$ at concentration of 1 mg mL^{-1} and analyzed at room temperature. GPC was carried out using a Waters high pressure liquid chromatography system equipped with Waters 1515 pump, 2414 differential refractive index detector and two connected Styragel columns. THF was used as the eluent with 0.02 M tetra-n-butylammonium fluoride trihydrate (TBAF) at a flow rate of 1 mL min^{-1} at room temperature. The synthesized PMVC-CTA had M_n = 8900 g mol^{-1}, M_w = 10000 g mol^{-1}, Đ = 1.12. Linear polystyrene standards were used for GPC calibration and polymer molecular weight were rounded to 100 g mol^{-1}. To synthesize a PMVC-PVPON diblock copolymer, PMVC macroinitiator (0.4 g, 0.04 mmol) was mixed with VPON monomer (1 g, 9 mmol) (the macroCTA was reacted at $[M]_0$/[CTA] ratio = 225/1) and AIBN (2 mg, 0.012 mmol; the [CTA]/[I] ratio = 3.3/1) in 1,4-dioxane solution (2.5 mL). The mixture was degassed with three cycles of freeze-pump-thaw followed by heating at 60 °C in oil bath for a desired time to obtain the desired molecular weight of the second polymer block. The synthesized block copolymers were purified and characterized as described above.

Turbidity Analysis. Temperature-dependent scattering intensity of polymer solutions was determined with fluorescence spectrophotometer (Varian, Cary Eclipse). The scattering intensity of 3 mL of polymer solutions (0.5 mg mL^{-1}) was analyzed at λ = 700 nm with temperature varied from 5 to 37 °C with the temperature rate of 0.2 °C per minute. To obtain polymer phase transition

temperatures, the curves of optical density as a function of temperature were analyzed using Origin Lab 2019 software to determine the curves' inflection points via differentiation.

Self-assembly of PMVC-PVPON polymersomes and DOX loading. The self-assembly of synthesized PMVC-PVPON diblock copolymers was carried out by dissolving 5 mg of a copolymer in 2 mL DI water followed by cooling down at 4 °C for 20 minutes and exposure to a room temperature for copolymer self-assembly. DOX-loaded $PMVC_{58}$-$PVPON_{65}$ polymersomes were prepared similarly. Briefly, 5 mg $PMVC_{58}$-$PVPON_{65}$ diblock copolymer was mixed with 2 mL of 1.5 mg mL^{-1} DOX solution at 4 °C in a refrigerator. After 20 minutes, the solution was brought to room temperature and dialyzed for 48 hours against 0.01 M phosphate buffer (pH = 7.2) using a dialysis bag with 8-10k Da MWCO (Fisher Scientific) to remove free DOX. For quantification of DOX loading capacity of (48.5 wt%), dialyzed DOX-loaded polymersomes were lyophilized and weighted. The encapsulated DOX was extracted by DI water and its amount was quantified via measuring DOX absorbance at λ = 490 nm using UV-vis spectroscopy. To determine the encapsulation efficiency of DOX after the drug encapsulation, free DOX was removed by dialysis in pH = 7.4 phosphate buffer (0.01 M phosphate). The collected buffer was freeze-dried and the residue of salt and free DOX was re-dissolved in DI water and quantified by UV-vis spectroscopy. The DOX loading efficiency was calculated as $(1-[m_f/m_t]) \times 100\%$, where m_f and m_t are the amounts of non-encapsulated free DOX and total mass of DOX, respectively.[57] The DOX-loaded liposomes were also prepared for animal study. The liposomes were prepared by hydration of thin films (EPC/DSPE-PEG2000, 23:16 mol%) with 2.5 mg mL^{-1} DOX and PBS (1X, HyClone) solutions, followed by sonication and stirring. The prepared liposomes were repeatedly extruded (25 °C) through polycarbonate filters with a pore diameter of 0.05 μm (Fisher Scientific, USA). The extruded liposomes were dialyzed in a 1 mL, ready-to-use dialysis tube

(MWCO at 3000 Da, Spectrum Labs) in PBS at 4 °C for 6 hours to remove free DOX. The loading amount was quantified based on the weight of DOX in liposomes and analyzed by UV-visible spectroscopy (Varian Cary 50, USA). Dialyzed DOX liposomes were freeze-dried and re-dissolved in chloroform to extract DOX. The extracted solution was analyzed using UV-vis spectroscopy and quantified based on a pre-established calibration curve. The liposome size (83 nm) was analyzed with DLS (Nano-ZS Zetasizer, Malvern). The average hydrodynamic particle size was determined from three independent runs.

Electron Microscopy. Transmission electron microscopy (TEM) images of the $PMVC_{58}$-$PVPON_{65}$ polymersomes were collected with a FEI Tecnai T12 Spirit TWIN TEM microscope operated at 80 kV. For sample preparation, 7 µL of polymersome solution (1 mg mL^{-1}) was dropped onto an argon plasma-treated Formavar/Carbon-coated copper grid (200 mesh, TED Pella) and after 60 s the excess solution was blotted off of the bottom of the grid with Kimwipe paper. The polymersomes were stained with 1% (wt) uranyl acetate for 10 s. Shape and morphology of the $PMVC_{58}$-$PVPON_{65}$ polymersomes were analyzed using FEI Quanta FEG scanning electron microscope (SEM) at 10 kV. A drop of aqueous polymersome solution was placed on a silicon wafer (5 mm x 5 mm). After overnight drying in a Petri dish, the specimen was sputter-coated with a 5-nm thick silver layer using Denton sputter-coater and imaged. For cryogenic electron microcopy (cryo-TEM), $PMVC_{58}$-$PVPON_{65}$ block copolymer (2 mg mL^{-1}) was self-assembled into vesicles as described above followed by extrusion through 0.1-µm pore size polycarbonate membrane using an Avanti mini-extruder (Avanti Polar Lipids, Inc). 3 µL of the extruded $PMVC_{58}$-$PVPON_{65}$ sample was applied to a glow-discharged 200 mesh Quantifoil R 2/1 grid (Electron Microscopy Sciences) followed by loading into the FEI Vitrobot Mark IV, where it was blotted and submerged into liquid ethane. A frozen grid was transferred to a Gatan 622 cryo-

holder and observed in an FEI Tecnai F20 electron microscope operated at 200 kV. Images were collected under low-dose conditions on a Gatan Ultrascan 4000 CCD camera.

Dynamic Light Scattering (DLS). DLS was performed using a Nano-ZS Zetasizer (Malvern) equipped with He-Ne laser (663 nm). The average hydrodynamic size of assemblies was obtained from three independent measurements of aqueous polymer solutions (2 mg mL^{-1}). The average hydrodynamic sizes of the self-assemblies were evaluated by fitting peaks of the intensity = f(size) curves using Origin Lab 2019 software, with the size standard deviation defined as the full width at half maximum. 300 μL of $PMVC_{58}$-$PVPON_{65}$ polymersomes (1 mg mL^{-1}) were incubated in 1mL of 10% FBS-containing PBS solution at 25 °C for 24 hours. The hydrodynamic size of the serum-treated $PMVC_{58}$-$PVPON_{65}$ polymersomes was determined using DLS.

Small-Angle Neutron Scattering (SANS). SANS measurements were performed with the EQ-SANS instrument at the Spallation Neutron Source (SNS, BL-6) at Oak Ridge National Laboratory (USA).[58] To cover the q-range needed, instrument configurations with sample-to-detector distance of 4 m (wavelength ~10 Å -13 Å) with instrument chopper setting at 60 Hz were used. The sample aperture was set to 10 mm in diameter. The polymersome sample was prepared by dissolving 3 mg of $PMVC_{58}$-$PVPON_{65}$ copolymer in 1 mL D_2O followed by cooling it down at 4 °C for 20 minutes and exposure to a room temperature for copolymer self-assembly. Before SANS measurement, the sample was diluted to 1mg mL^{-1} followed by vortexing. The measurement was carried out with 600 μL of sample in 2 mm Banjo cell. The sample temperature was controlled by a water bath. The neutron wavelengths were converted from the time-of-flight and then were used to reduce data into reciprocal q space, where $q = 4\pi\sin(\theta)/\lambda$; 2θ is the scattering angle, and λ is the neutron wavelength. The conversion and other reduction procedures such as normalization for incident flux spectrum, sample transmission, detector sensitivity, the detector

dark current and azimuthal average were performed with the facility-provided data reduction software Mantid. NIST SANS data analysis packages in Igor Pro[59] were used for data analysis. Fit quality was determined by minimizing the goodness-of-fit parameter (χ^2), and parameters were constrained to physically reasonable values of size and thickness and consistency with other measurements, such as DLS and TEM.

The data was quantitatively analyzed by performing a modified Guinier analysis.[60,61] At larger q, corresponding to smaller length scales, where the thickness is much smaller than the overall size of the polymersome, the curvature of the polymersome becomes unimportant; instead it can be viewed as a sheet with a thickness d. For $qR_g < 1$, where R_g is related to the thickness as $d = (12)^{1/2} R_g$, the intensity of scattering from a sheet goes as

$$I(q) \propto \frac{1}{q^2} e^{-q^2 Rg^2} \qquad (1)$$

Therefore, from fitting $\ln(I(q)q^2)$ versus q^2, $-R_g^2$ can be derived from the slope from which the thickness can be calculated.

The Guinier-Porod modelwas applied to obtain the overall size, R_{g1} of the polymersomes.[62] The scattering intensity I(q) is given as

$$I(q) = I_0 e^{-\frac{q^2 Rg1^2}{3-s}} \qquad (2)$$

where R_{g1} is the radius of gyration of the particles, and *s* is the dimension variance.

Release from DOX-loaded PMVC$_{58}$-PVPON$_{65}$ polymersomes. The release of DOX from DOX-loaded PMVC$_{58}$-PVPON$_{65}$ polymersomes was tested using dialysis. For that, 1.5 mL of DOX-loaded PMVC$_{58}$-PVPON$_{65}$ polymersome solution was placed in a Float-A-Lyzer dialysis tube (3000 Da MWCO, Spectrum Laboratories) which was immersed in 50 mL of PBS buffer

solution (HyClone) at either pH = 7.4 or pH = 5 and kept under stirring (80 rpm) at 37 °C in an incubator (Precision Scientific Company). The PBS solution (3 mL) was withdrawn periodically and analyzed using UV-visible spectroscopy to quantify the amount of DOX released.

Animal Experiments. All animal procedures were conducted according to the 'Guide for the Care and Use of Laboratory Animals' and were approved by the Institutional Animal Care and Use Committees at the University of Alabama at Birmingham.

Survival Analyses. Two-month old male C57BL/6J mice were used for the experiment. The C57BL/6J mice were randomized into subgroups with saline as a vehicle (0.9% NaCl in water) for the control group. 15 mg/kg/week of DOX as high dose was used for non-survival. DOX encapsulated into liposomes and polymersomes were labeled as Lipo-DOX and Poly-DOX, respectively. All the doses of DOX were given to mice via intra-peritoneal injection. The mortality rate in each group was checked every day.

Gravimetric analysis. Mice were anesthetized with 2% isoflurane in an oxygen mix and injected with 4 IU/g heparin as previously reported.[63] The lungs, left ventricle (LV), and spleen were separated and weighed individually.

Statistical analysis. All data is expressed as mean ± standard mean error. Statistical analyses ($p<0.05$) were performed using Graph 205 Pad Prism 7. Analysis of variance (ANOVA)-one way was used. $p < 0.05$ was considered as statistically significant.

RESULTS AND DISCUSSION

Synthesis of PMVC-PVPON diblock copolymers. To prepare a hydrophobic PMVC block, first, (3-methyl-N-vinylcaprolactam) (MVC) monomer was synthesized by alkylation α-H of vinyl caprolactam monomer as shown in Figure 1a as we reported earlier.[49] The PMVC macroinitiator

was obtained by RAFT polymerization using O-ethyl-S-(1-methoxycarbony) ethyl dithiocarbonate as a chain transfer agent after 6-hour reaction (Figure 1b). The number-average molecular weight (M_n) of PMVC analyzed using GPC was found to be M_n = 8900 g mol^{-1} with the polydispersity of Đ =1.12 (Figure S1). Unlike earlier reported methylated polyvinylpyrrolidone homopolymers poly(3-methyl-N-vinyl-2-pyrrolidone) and poly(3,3-dimethyl-N-vinyl-2-pyrrolidone), which display a cloud point at 64 and 41 °C, respectively,[64] we found that the methylated poly(N-vinylcaprolactam) counterpart, PMVC, was not soluble in water at temperatures above 4 °C because of the increased hydrophobicity due to the additional methyl substitute to the caprolactam ring. The ^{1}H NMR analysis of PMVC shows the presence of the broad signals at 4.4 ppm (b: 1H) which can be used for molecular weight analysis of the PMVC-PVPON diblock copolymers (Figure 2).

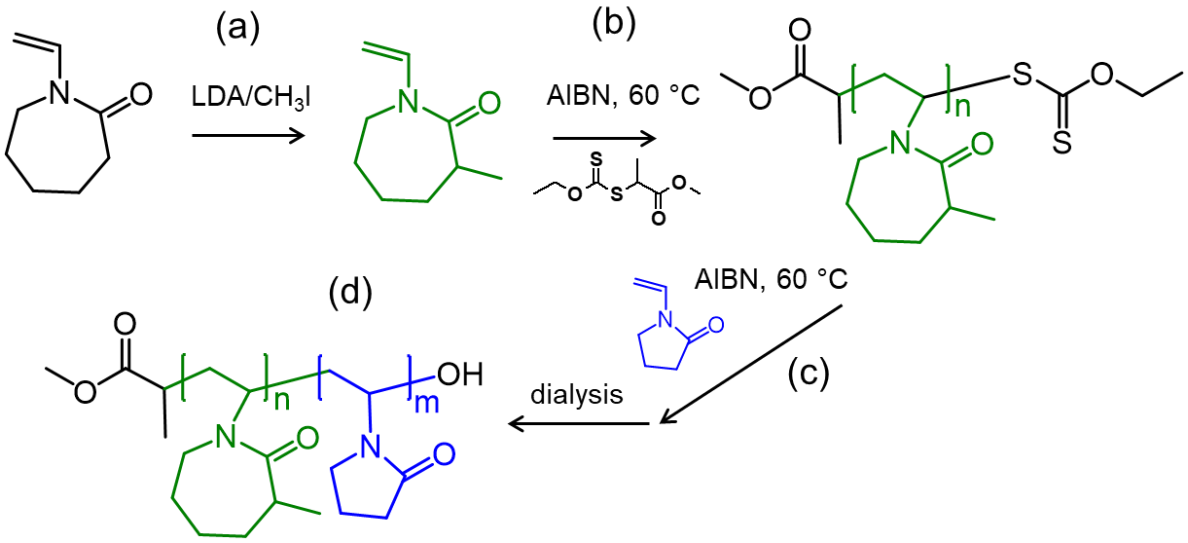

Figure 1. Synthesis of $PMVC_n$-$PVPON_m$ diblock copolymer using RAFT copolymerization.

The hydrophilic second block of PVPON was further synthesized using PMVC as the RAFT macroinitiator by controlling the reaction time (Figure 1c) for 3, 5, 8 hours. The block copolymer molecular weight and composition were characterized using GPC and ^{1}H NMR analyses. The M_n values of the synthesized PMVC-PVPON diblock copolymers were calculated using the integration ratio between the areas of 3.4 - 4.1 ppm (PVPON) and 4.2 - 4.7 ppm (PMVC).[49,65] By gradually increasing the content of PVPON in diblock copolymers, integration area of –CH- group in PVPON (3.4 - 4.1 ppm), increased accordingly and was utilized for monitoring the PVPON chain growth. The integration ratio of the distinguishable characteristic peaks from poly(N-vinylcaprolactam) PVCL and PVPON to quantify the compositions of statistical block copolymers of (PMVC-co-PVCL)-b-(PVPON-co-PMVC) and PVCL-b-PVPON was previously reported.[48] The chemical shift of –CH- group in the PMVC backbone is close to PVCL and is mainly dependent on the lactam ring, therefore, the alkylation of α-H would not influence the chemical shift significantly. The length of the PVPON block in the synthesized $PMVC_m$-$PVPON_n$ was calculated to be n = 20, 65, and 98 for 3-, 5-, 8-hour reaction time, respectively, based on the NMR data (Figure 2; Table 1). The GPC traces in THF showed a series of unimodal distributions with various elution times (Figure S1). Table 1 shows that the copolymers had low polydispersity indices ranging from Đ = 1.12 for $PMVC_{58}$-$PVPON_{20}$ to Đ = 1.17 for $PMVC_{58}$-$PVPON_{98}$ indicating the uniform control of polymer growth.[66] The GPC number-average molecular weights were slightly lower than that calculated from ^{1}H NMR data but in the similar range (Table 1). The observed small difference between the average molecular weights of the copolymers obtained by GPC can be due to different solubility of PMVC and PVPON in THF. While THF is a good solvent for the hydrophobic PMVC, and therefore a reliable GPC analysis of PMVC-CTA molecular weight can be carried out, the poor solubility of PVPON in this solvent[67] can result in

highly coiled conformation of PVPON blocks attached to the PMVC block, which can lead to underestimated hydrodynamic volumes of the copolymers measured by GPC and therefore lower the average molecular weights.[68]

Table 1. Number-Average Molecular Weights (M_n), Polydispersity (Đ), and Chemical Composition of the Polymers.

Polymer	***M*n (¹H NMR), Da**	***M*n (GPC)[a], Da**	***M*w (GPC), Da**	**Đ (GPC)**	**PMVC, wt%**	**PMVC:PVPON ratio**
$PMVC_{58}$		8900	10000	1.12	100	1:0
$PMVC_{58}$-$PVPON_{20}$	11100	9600	11000	1.14	80	1:0.34
$PMVC_{58}$-$PVPON_{65}$	16200	9900	11300	1.14	55	1:1.12
$PMVC_{58}$-$PVPON_{98}$	19700	10100	11900	1.17	45	1:1.67

[a]The GPC number-average molecular weights were obtained using polystyrene linear standards.

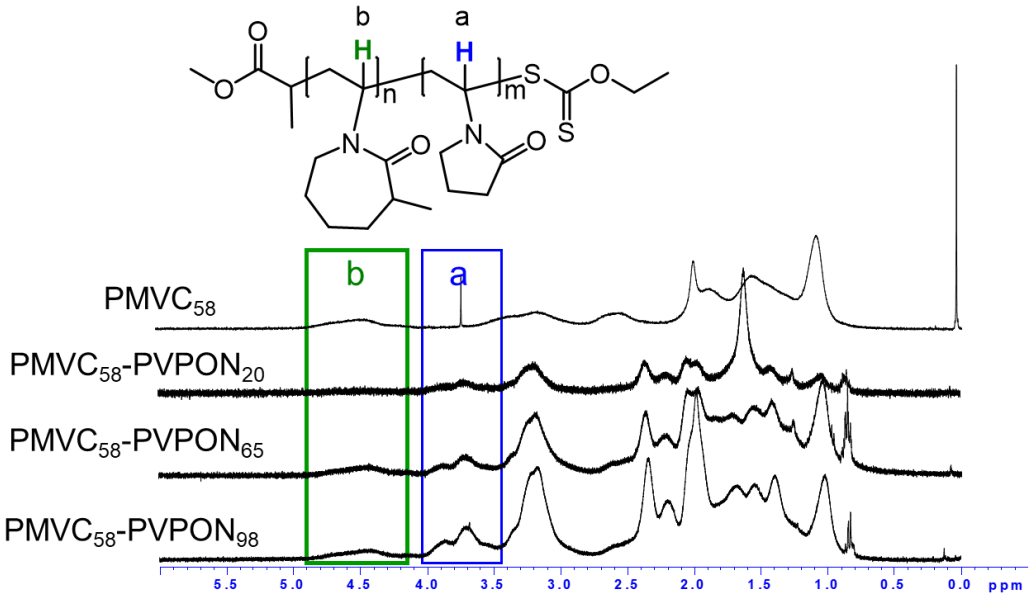

Figure 2. ¹H NMR spectra of the $PMVC_n$ homopolymer (n = 58) and $PMVC_{58}$-$PVPON_m$ diblock copolymers with m = 20, 65, 98.

Temperature response of PMVC-PVPON diblock copolymers. The increased hydrophobicity of PMVC due to the monomer methylation resulted in the PMVC insolubility in aqueous solutions at temperatures above 4 °C unlike its less hydrophobic homologue PVCL, which is soluble in water at temperatures lower than its LCSTs that can range from 36 to 50 °C depending on the molecular weight, polymer concentration, and added functionalities.[51,69] Similarly, introduction of a bulky hydrophobic *tert*-butyl on the caprolactam ring in PVCL copolymers was shown to vary LCST by inducing dehydration of repeating units even at temperatures lower than the LCST.[70] Gradually increasing hydrophobicity of the alkyl groups from methyl to ethyl and propyl in N-vinylpyrrolidone was reported to decrease the cloud points of the corresponding alkylated PVPON homopolymers from 64 to 25 and to below 0 °C, respectively, while non-modified PVPON is soluble in water and does not display any cloud point at a temperature range from 10 to 80 °C.[64,71]

The addition of the hydrophilic PVPON block was earlier reported to increase the hydrophilicity of PVCL-PVPON diblock copolymers and their corresponding cloud points from 39 °C for $PVCL_{155}$ to 42.5 °C for $PVCL_{155}$-$PVPON_{164}$ and to 46.5 °C for $PVCL_{155}$-$PVPON_{785}$.[48] Herein, all synthesized $PMVC_{58}$-PVPON block copolymers became soluble in water at temperatures above 10 °C (Figure 3). The turbidimetric analysis in Figure 3 shows that the synthesized $PMVC_{58}$-$PVPON_n$ block copolymers solutions exhibited reversible temperature-dependent optical density. The 0.5 mg mL^{-1} aqueous copolymer solutions were stored at 4 °C before measurements to maintain complete solution transparency. The optical densities were monitored with fluorometry at λ = 700 nm as a function of temperature.[65] For $PMVC_{58}$-$PVPON_n$ block copolymers, increasing the molecular fraction of PVPON from n = 20 to n = 65, and to n = 98, caused the copolymer's LCST temperature, defined as a 50% decreased solution transparency

and obtained as the inflection point of the temperature-dependent optical density curves, to increase from 15.2 °C (Figure 3a) to 18.6 °C (Figure 3b) and to 19.2 °C (Figure 3c), respectively, reflecting the increased hydrophilic portion of the copolymer. The optical density increase reflects the continuous copolymer phase change associated with the coil-to-globule transition of the polymers. As the content of PVPON increases, the LCST value shifts to a higher temperature where the block copolymer phase transition occurs.[48,49,72] Noteworthy, the $PMVC_{58}$-$PVPON_{20}$ block copolymer with the lowest PVPON content (~20%) exhibits a sharp intensity change which spans a temperature range of five degrees from 13 to 18 °C (Figure 3a), while a slower optical density increase is observed for the block copolymer with a larger PVPON content, spanning a range of nine degrees from 14 to 23 °C for $PMVC_{58}$-$PVPON_{65}$ (Figure 3b) and from 14 to 24 °C for $PMVC_{58}$-$PVPON_{98}$ (Figure 3c).

Similarly, a dependence of the shape of the phase transition profiles on the copolymer molar composition was reported for poly(3-(*tert*-butoxycarbonylmethyl)-N-vinyl-2-caprolactam)-stat-N-vinyl-2-caprolactam)random copolymers, where increased copolymer hydrophobicity was due to an increased molar ratio of a hydrophobic *tert*-butyl side group, resulted in sharper phase transition on heating.[70] The steeper slopes for the optical density increase upon heating were also observed for $PVPON_{128}$-$PVCL_n$ diblock copolymers when the PVCL chain length increased from n = 81 to n = 165 and to n = 281.[48]

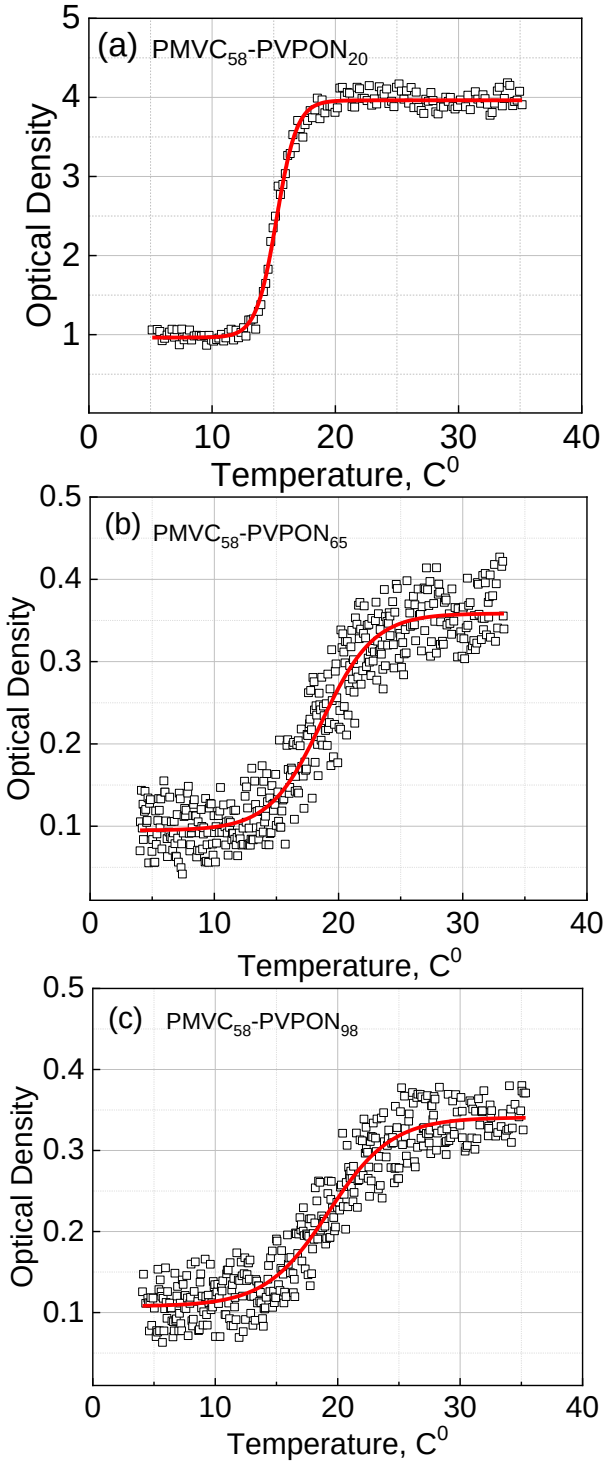

Figure 3. Turbidimetric analysis of (a) $PMVC_{58}$-$PVPON_{20}$ (b) $PMVC_{58}$-$PVPON_{65}$ and (c) $PMVC_{58}$-$PVPON_{98}$ diblock copolymer solutions. Scattering experiments were performed using fluorometry at λ= 700 nm with 0.5 mg mL^{-1} aqueous block copolymer solutions. The analysis was carried out at 0.2 °C heating step with the temperature rate of 0.2 °C min^{-1}, with three measurements for each step.

Self-assembly of $PMVC_{58}$-$PVPON_n$ diblock copolymers. The temperature-responsive $PMVC_{58}$-$PVPON_n$ block copolymers were self-assembled from 2.5 mg mL^{-1} polymer solutions, which were first cooled down at 4 °C for 20 minutes to achieve complete copolymer molecular dissolution followed by exposure to room temperature (T ≥ 25 °C). Heating of $PMVC_{58}$-$PVPON_{20}$ resulted in a drastic increase of the solution optical density (Figure 3a) and a formation of large precipitates greater than 1-3 μm as observed with DLS (not shown). This result implies that a relatively low hydrophilic content of PVPON in the copolymer is not enough to effectively stabilize the PMVC nanoassemblies in solution leading to their aggregation and precipitation. In contrast, the average size of the $PMVC_{58}$-$PVPON_{65}$ and $PMVC_{58}$-$PVPON_{98}$ block copolymer self-assemblies was 370 ± 155 nm and 220 ± 90 nm, respectively, as measured by DLS (Figure 4). The 41%-decrease in the average size of $PMVC_{58}$-$PVPON_{98}$ nanoparticles compared to that of the copolymer with a shorter PVPON (n = 65) is in good agreement with previous reports on the reduced size of a self-assembled particle due to increasing steric repulsions of longer hydrophilic chains in the particle hydrophilic corona.[48,56,65,73] In contrast to our previous studies with PVCL-PVPON block copolymers, where the copolymer self-assembly can be initiated at temperatures greater than 40 °C, the herein reported $PMVC_{58}$-$PVPON_{65}$ and $PMVC_{58}$-$PVPON_{98}$ block copolymers can facilitate the self-assembly process already at room temperature due to the extremely low LCST of the PMVC block (Table 1).

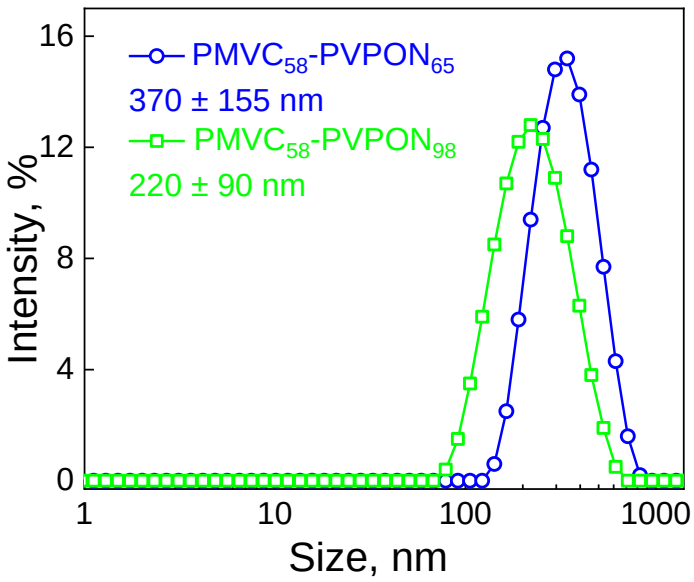

Figure 4. Size of $PMVC_{58}$-$PVPON_{98}$ (squares) and $PMVC_{58}$-$PVPON_{65}$, (circles) diblock copolymer polymersomes as measured by DLS at 25 °C. Self-assembly was carried out by exposure of 2 mg mL^{-1} copolymer aqueous solutions first to 4 °C for 20 min followed by exposure to 25 °C.

Figure 5 shows TEM images of the polymeric nanoparticles obtained via self-assembly of $PMVC_{58}$-$PVPON_{98}$ (Figure 5a) and $PMVC_{58}$-$PVPON_{65}$ (Figure 5b) block copolymers. The images show that both copolymers produced spherical polymersome morphologies upon self-assembly with a relatively narrow size distribution of 230 ± 31 nm and 300 ± 25 nm for $PMVC_{58}$-$PVPON_{98}$ and $PMVC_{58}$-$PVPON_{65}$, respectively, which is in good agreement with the DLS data (Figure 4). The hollow cavity inside nanoparticle interiors seen from the TEM images confirmed the polymersome morphology of the nanoparticles.

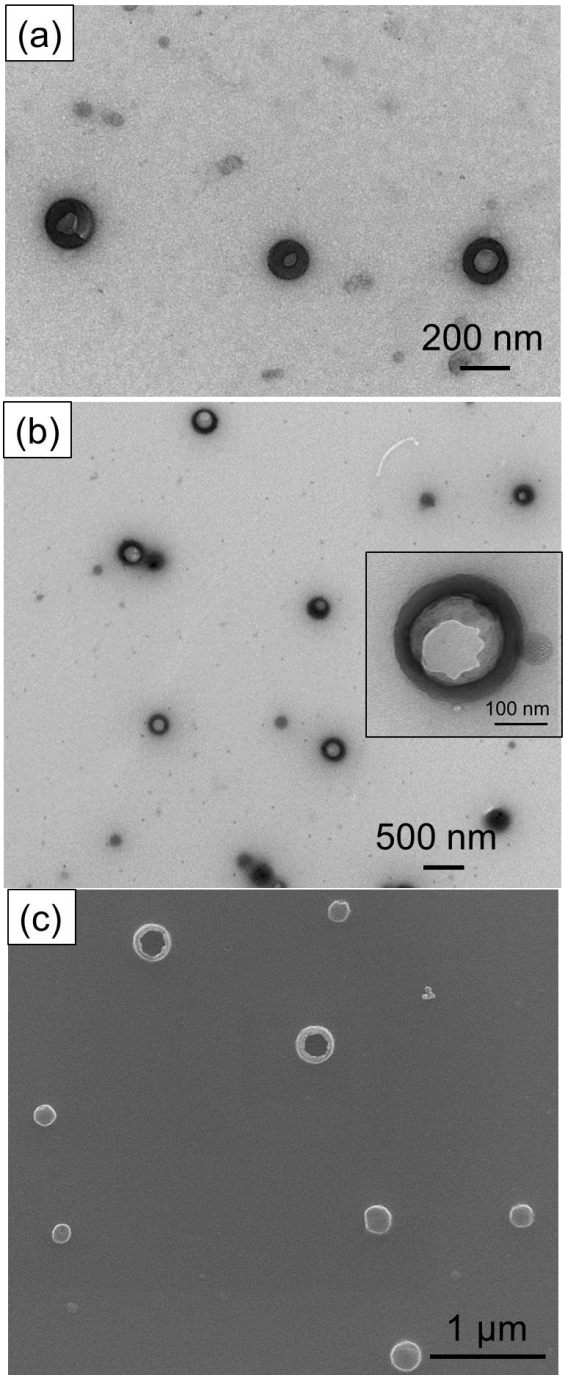

Figure 5. TEM images of (a) $PMVC_{58}$-$PVPON_{98}$ and (b) $PMVC_{58}$-$PVPON_{65}$ diblock copolymer polymersomes. (c) SEM image of $PMVC_{58}$-$PVPON_{65}$ diblock copolymer polymersomes.

Moreover, the nanocapsule structure of the assemblies is evident from the SEM images of $PMVC_{58}$-$PVPON_{65}$ polymersomes shown in Figure 5c where larger particles became concave upon drying, leaving behind the hemispherical nanocapsule shape. The estimation of shell thickness from the SEM analysis resulted in an average dry wall thickness of 18 ± 2 nm which is similar in range to the 19- nm shell thicknesses reported for poly(N-vinylcaprolactam)$_{21}$-*block*-poly(dimethylsiloxane)$_{65}$-*block*-poly(N-vinylcaprolactam)$_{21}$ ($PVCL_{21}$-$PDMS_{65}$-$PVCL_{21}$) triblock copolymer polymersomes as measured by SANS in solution at T = 25 °C.[73]

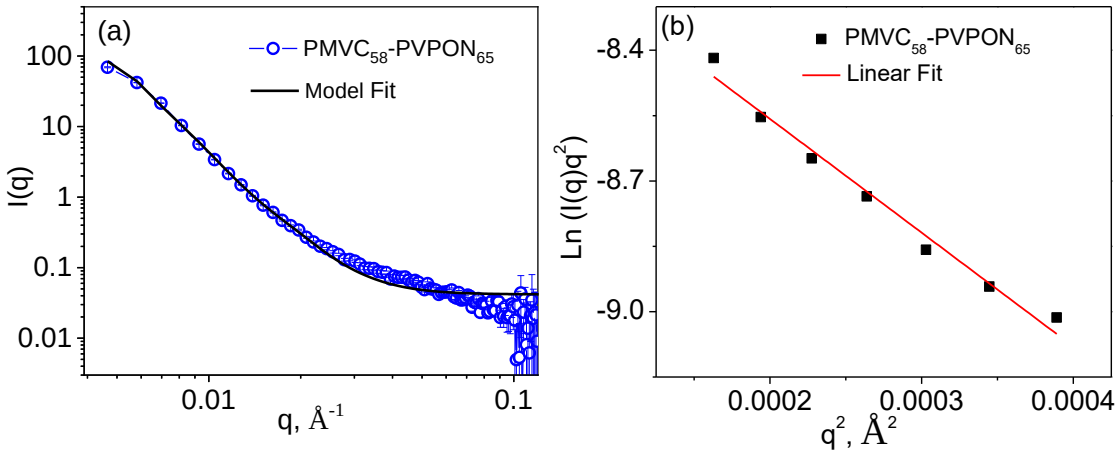

Figure 6. (a) SANS curve of $PMVC_{58}$-$PVPON_{65}$ polymersomes (circles) at 25 °C and its fit by the Guinier-Porod model (black solid line) showed an R_g of 123 nm. (b) Modified Guinier plot of the $PMVC_{58}$-$PVPON_{65}$ vesicles (squares). The red solid line is a linear fit to the data, giving a slope of -2612.8 $Å^2$, corresponding to a membrane thickness of 17.7 ± 2.2 nm.

The self-assembly of $PMVC_{58}$-$PVPON_{65}$ copolymer was also analyzed by SANS. The Guinier-Porod model was used to calculate the overall radius of gyration R_g, the dimension variance which distinguishes spherical, rod-like or plates shapes, and the Porod exponent which describes the particle shape (Figure 6a). A dimension variance of 0.1 was obtained from the model fit, which

being close to zero describes a 3D globule shape of a vesicle. At the higher q range, the Porod exponent was found to be 3.78, which is slightly lower than 4 (the surface of a smooth sphere) and implies surface roughness due to coiled polymer chains extending from the membrane surfaces.[59] The model fit resulted in R_g of 123 nm which is in agreement with the hydrodynamic radius (R_h) calculated by DLS (259 nm/2 = 129.5 nm; Figure S2) resulting in the ratio of R_g/R_h = 0.946 which is close to 1 indicating a hollow sphere with a thick shell. In the modified Guinier plot (Figure 6b), the slope of a linear fit to the data is equal to $-R_g^2$ and was found to be -2612.8 ± 157.6 Å^2, from which the polymersome shell thickness was calculated to be 17.7 ± 2.2 nm, which is similar to that obtained from the SEM (Figure 5c) and cryo-TEM analysis (~17 nm; Figure S3).

Since polymersomes are soft and fluid-like vesicles, we have explored the time-dependent size stability of the self-assembled vesicles. Figure 7a shows that the average size of the $PMVC_{58}$-$PVPON_{65}$ polymersomes stored at room temperature for 50 days was 345 ± 90 nm and did not display any significant dimension changes with time as measured by DLS at room temperature. This result shows an exceptional morphological stability of the $PMVC_{58}$-$PVPON_{65}$ vesicles unlike previously reported poly(lactic acid)-*block*-poly(ethylene glycol) and poly(2-methyl-oxazoline)-block-poly(dimethylsiloxane)-*block*-poly(2-methyl-oxazoline) block copolymer polymersomes that were shown to undergo size increases due to fusion after self-assembly.[74,75,76] It is worth noting that temperature was the only trigger required for the self-assembly of PMVC-PVPON unilamellar vesicles unlike methods involving solvent switching followed by dialysis, or a thin-film rehydration method necessary to assemble a majority of amphiphilic block copolymers.[75]

Loading and release of DOX using $PMVC_{58}$-$PVPON_{65}$ polymersomes. Hydrophilic DOX hydrochloride was encapsulated into $PMVC_{58}$-$PVPON_{65}$ polymersomes by mixing 1.5 mg mL^{-1} DOX solution at 4 °C followed by exposure of the mixture to a room temperature and dialysis

against 0.01 M phosphate buffer at pH = 7.2. The DOX loading capacity was found to be 49 wt % resulting in the polymersome size of 346 ± 25 nm as measured by DLS (Figure 7b).

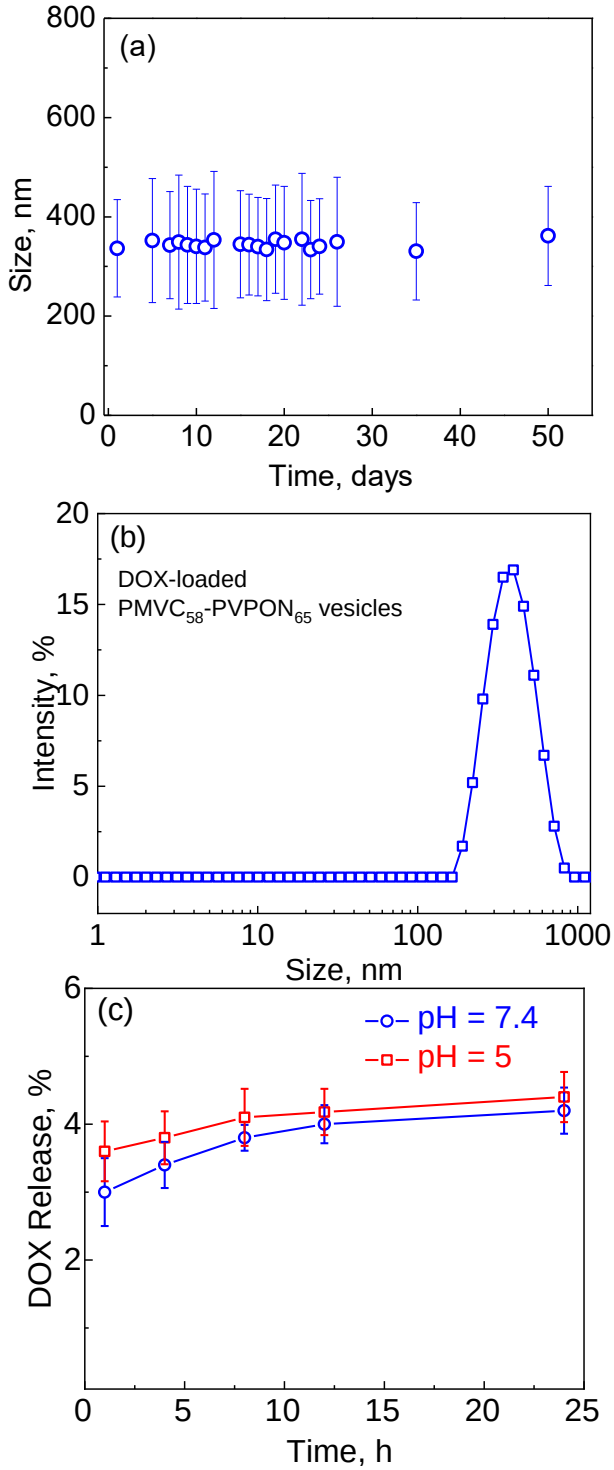

Figure 7. (a) Time-dependent hydrodynamic size variations of DOX-free $PMVC_{58}$-b-$PVPON_{65}$ polymersomes measured for 50 days, and (b) hydrodynamic size of DOX-loaded $PMVC_{58}$-b-$PVPON_{65}$ polymersomes after 24 hours as measured by dynamic light scattering. (c) Time-dependent release of DOX (%) from DOX-loaded $PMVC_{58}$-$PVPON_{65}$ polymersomes at pH = 7.4 and pH = 5 as measured by UV-vis spectroscopy.

The encapsulation efficiency of DOX loading was found to be 95% with the drug loading concentration of 1.5 mg mL^{-1}. In comparison to the previously reported $PVCL_n$-$PDMS_{65}$-$PVCL_n$ polymersomes with 40% loading capacity,[65] or amphiphilic graft polyphosphazene polymersomes with the highest loading content of 16%,[77] or 6% loading content achieved by poly(trimethylene carbonate)-*block*-poly(L-glutamic acid), [78] the herein developed $PMVC_{58}$-$PVPON_{65}$ polymersomes exhibit both an exceptionally higher loading capacity (LC = 49%) and encapsulation efficiency (95%) due to a temperature-facilitated spontaneous loading of the drug and hydrophobic interactions between drug molecules and $PMVC_{58}$-$PVPON_{65}$ chains. Indeed, in our previous work, poly(3-methyl-N-vinylcaprolactam)-based block copolymer micelles demonstrated increased Nile Red dye loading from 27 to 35% (w/w) when temperature increased from 26 to 50 °C. [49] Due to the hydrophobic interactions between the dye and the copolymer chains, the chain-chain interactions were decreased and the phase transition temperature for the Nile Red-loaded micelles appeared at a slightly higher temperature than that for the empty micelles.[49]

As shown in Figure 7c, a negligible amount of DOX release was observed when the DOX-loaded $PMVC_{58}$-$PVPON_{65}$ polymersomes were exposed to 0.01 M buffer solutions at pH = 7.4 or pH = 5 for 24 hours. Moreover, no significant increase of DOX in solution (below 5%) was observed after 30 days of dialysis at room temperature. This is an important observation as the

majority of thermosensitive liposomes developed for delivery of DOX to tumors, although demonstrated a low leakage of DOX at 37 °C in in vitro assays, showed a burst release of DOX upon injection and high DOX leakage in blood within the first hour of injection.[24,79,80] Therefore, in contrast to unavoidable leakage observed in many liposomal delivery systems whose morphological stability relies on temperature, pH and chemistry of lipids, PMVC-PVPON polymersomes were found to be resistant to pH changes and exhibited a superior stability against DOX leakage at physiological conditions.

Moreover, the $PMVC_{58}$-$PVPON_{65}$ polymersomes demonstrated an excellent structural stability in serum. The hydrodynamic size of the $PMVC_{58}$-$PVPON_{65}$ polymersomes incubated in 1 mL of 10% FBS-containing PBS solution at 25 °C for 24 hours did not showed any significant size increase or any signs of aggregation as determined using DLS and TEM (Figure S4). This can be explained by the presence of hydrophilic PVPON inner and outer coronas that can inhibit protein adsorption and cell recognition similarly as poly(ethylene glycol) (PEG).[81,82] PEG has been long used to modify liposomes for their stealth behavior in blood to increase their circulation time.[83,84] Due to its high hydrophilicity, similar to PEG, PVPON could prevent protein absorption on particle surfaces and affect phagocytosis of PVPON-coated polymeric particles *in vivo*.[81,82] The amount of PVPON-coated particles trapped in the reticuloendothelial system organs was also reported to be less than those coated with PEG.[82] We have also shown that the presence of PVPON as an outer layer in hydrogen-bonded (tannic acid/PVPON) multilayer capsules rendered them highly stable in serum and did not affect their ultrasound sensitivity in vitro or *in vivo*.[85,86]

Cardiotoxicity of DOX loaded into liposomes and $PMVC_{58}$-$PVPON_{65}$ polymersomes. The high dose of 15 mg kg^{-1} $week^{-1}$ DOX has been demonstrated to be a non-survival toxic dose of the drug with 100% mice mortality (n = 10) within 14 days of treatment (Figure 8). The saline injected

mice (n = 9) were used as a non-toxic vehicle control and demonstrated 100% survival rate (Figure 8). These saline-injected mice were used in comparison to the mice treated with DOX encapsulated into liposomes (Lipo-DOX; n = 8) or polymersomes (Poly-DOX; n = 9) with the final injection dose of 15 mg kg^{-1} $week^{-1}$ DOX. In contrast to the non-encapsulated DOX that led to 100% mice mortality, all mice injected with Lipo-DOX or Poly-DOX survived the treatment, indicative of non-toxicity to the animals after the 14-day treatment (Figure 8).

However, the gravimetric analyses of the animal organs revealed that the Lipo-DOX injection resulted in atrophic toxicity showing as statistically significant decrease in the body weight compared to Poly-DOX and saline-naive control (Table 1). Furthermore, gravimetric analyses of the left ventricle, lung, and spleen masses demonstrated a reduction in the lung and spleen masses normalized with the body mass ($p<0.05$) in the Lipo-DOX treated mice compared to the saline non-toxic control (Table 1). In contrast, no significant decrease in the masses of the left ventricle, spleen or lung masses was observed for the Poly-DOX treated mice (Table 1). As reported previously in the study with mice injected with non-encapsulated low 7.5 mg kg^{-1} $week^{-1}$ DOX dose, where 70% of mice survival was observed after 14 days of treatment, the decrease in the normalized left ventricle, lung and spleen masses was indicative of splenocardiac cachexia which was accompanied by myocyte deterioration and myocardium damage.[7]

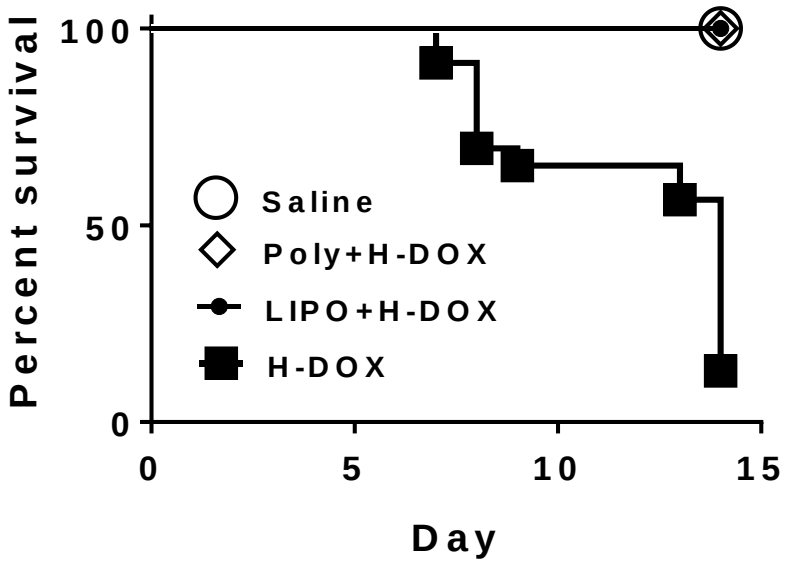

Figure 8. Survival rate in mice injected with saline (control), high dose (15 mg kg^{-1} $week^{-1}$) of non-encapsulated DOX (H-DOX), and DOX encapsulated in liposomes (Lipo-DOX), or in polymersomes (Poly-DOX) and analyzed by a log-rank test ($p < 0.01$ vs saline control).

Table 2. Gravimetric and necropsy parameters in Lipo-DOX and Poly-DOX groups (high dose of DOX 15 mg kg^{-1}) compared to the saline control.

Parameters	**Saline**	**Lipo-DOX**	**Poly-DOX**
Sample size	n=9	n=8	n=9
Body weight, g	24±1	21±1*	23±1
Left ventricle, mg	74±8	62±7*	71±9
Left ventricle/body weight, mg/g	3.07±0.2	2.97±0.2	3.11±0.2
Lung mass (dry), mg	33±5	26±3.0*	33±4
Spleen, mg	64±5	49±9*	61±5
Spleen/body weight, mg/g	2.6±0.2	2.3±0.3*	2.7±0.2

Values are averages ± standard errors. Data were analyzed by one-way ANOVA. *p<0.05 versus the saline control.

CONCLUSIONS

We synthesized poly(N-vinylpyrrolidone)-*block*-poly(3-methyl-N-vinylcaprolactam) (PVPON-PMVC) temperature-responsive diblock copolymers and demonstrated their self-assembly into nanosized polymersomes at room temperatures from aqueous solutions. The DLS data revealed that the cloud point of $PMVC_m$-$PVPON_n$ copolymers is below 20 °C. The phase transition of the $PMVC_{58}$-$PVPON_n$ copolymer was varied from 19.2 to 18.6 and to 15.2 °C by decreasing the length of the hydrophilic $PVPON_n$ block from n = 98 to n = 65, and to n = 20. The copolymers assembled into stable vesicles at room temperature when PVPON polymerization degree was 65 and 98 as demonstrated by DLS, TEM and SANS analyses. Unlike many liposomal, micellar or synthetic drug delivery systems, these polymersomes exhibit an exceptionally high loading capacity of DOX (49%) and encapsulation efficiency (95%) due to spontaneous loading of the drug at room temperature from DOX aqueous solution because of hydrophobic interactions between the polymer blocks and the drug. Moreover, the $PMVC_{58}$-$PVPON_{65}$ polymersomes displayed an excellent structural stability in serum. We also showed that while injecting C57BL/6J mice with the lethal dose of DOX at 15 mg kg^{-1} resulted in 100% mortality within 14-day treatment period, the DOX-loaded $PMVC_{58}$-$PVPON_{65}$ polymersomes showed 100% survival of mice indicating that the polymersomes can be used for successful DOX entrapment. The gravimetric analyses of the animal organs from mice treated with DOX encapsulated into liposomes and $PMVC_{58}$-$PVPON_{65}$ polymersomes revealed that the Lipo-DOX injection caused some toxicity manifesting by the decreased body weight compared to Poly-DOX and a saline control. Moreover, the gravimetric analyses of the left ventricle, lung, and spleen masses demonstrated a reduction in the lung and spleen masses in the Lipo-DOX treated mice compared to the non-toxic saline control. In contrast, no significant decrease of those masses was observed for the Poly-DOX treated mice. Our results provide evidence for superior stability of these synthetic polymersomes *in vivo* to be developed

into advanced therapeutics carriers with minimal side effects. Importantly, the innovative aspects of the reported polymersomes lie in their ability to easily load anticancer therapeutics from aqueous phases without using organic solvents due to the LCST of PMVC lower than 4 °C, which may be beneficial for encapsulation of peptide-based and RNA-based therapeutics; as well as in the polymersomes much higher encapsulation efficiency and drug loading unlike many other currently developed block copolymer-based nanocarriers. Also, the presence of poly(vinylpyrrolidone) in the outer polymersome corona allows for high inherent hydrophilicity of the vesicles resulting in their good stability in serum which has been reported to successfully prevent protein adsorption and affect phagocytosis similar to or better than PEG. Furthermore, as demonstrated in this work, the vesicle size can be easily decreased down to 100 nm by using membrane extrusion, which can be helpful in passive tumor targeting through the enhanced permeation and retention (EPR) effect due to leaky cancerous endothelium. These aspects of the reported block copolymer system make it worth of further insight into the release mechanism from these polymersomes through incorporation of degradable ester or disulfide intracellular degradable linkages between the two blocks through the use of either acid RAFT agents[87] or disulfide coupling to prepare a PMVC macro-RAFT agents from a RAFT agent with pyridyl disulfide functionality and PVPON thiol.[88]

ASSOCIATED CONTENT

Supporting Information

The Supporting Information is available free of charge on the ACS Publications website: GPC traces of PMVC and PMVC-PVPON diblock copolymers and DLS of $PMVC_{58}$-$PVPON_{65}$ diblock copolymer polymersomes in D_2O and in serum solution. TEM and cryo-TEM of $PMVC_{58}$-$PVPON_{65}$ diblock copolymer polymersomes.

AUTHOR INFORMATION

Corresponding Author
*E-mail: ekharlam@uab.edu.

Notes
The authors declare no competing financial interest.

ACKNOWLEDGMENTS

This work was supported by NSF-DMR 1608728 (E.K.). UAB transmission electron microscopy facility and UAB High Resolution Imaging facility (Scanning Electron Microscopy) are also acknowledged. The cryo-EM work was carried out in the UAB Cryo-EM facility (UAB Department of Microbiology). Neutron scattering research used resources at Spallation Neutron Source, a DOE Office of Science User Facility operated by the Oak Ridge National Laboratory. The Office of Biological and Environmental Research of the US DOE is also acknowledged (S. Q). Will Higgins (UAB) is acknowledged for technical assistance.

REFERENCES

(1) Khasraw, M.; Bell, R.; Dang, C. Epirubicin: Is it like doxorubicin in breast cancer? A clinical review. *Breast* **2012**, *21*, 142-149.

(2) Sawyer, D. B. Anthracyclines and Heart Failure. *N. Engl. J. Med*. **2013**, *368*, 1154-1156.

(3) Zhu, W.; Shou, W.; Payne, R. M.; Caldwell, R.; Field, L. J. A Mouse Model for Juvenile Doxorubicin-Induced Cardiac Dysfunction. *Pediatr. Res*. **2008**, *64*, 488-494.

(4) Chatterjee, K.; Zhang, J.; Honbo, N.; Karliner, J. S. Doxorubicin cardiomyopathy. *Cardiology* **2010**; *115*, 155-162.

(5) Volkova, M.; Russell R 3rd. Anthracycline cardiotoxicity: prevalence, pathogenesis and treatment. *Curr. Cardiol. Rev*. **2011**, *7*, 214-220.

(6) Hong, Y. J..; Park, H. S.; Park, J. K.; Han, K.; Park, C. H.; Kim, T. K.; Yoo, S. J.; Lee, J. Y.; Kim, P. K.; Hur, J.; Lee, H.-J.; Kim, Y. J.; Suh, Y. J.; Paek, M. Y.; Choi, B. W. Early Detection and Serial Monitoring of Anthracycline-Induced Cardiotoxicity Using T1-mapping Cardiac Magnetic Resonance Imaging: An Animal Study. *Scientific Rep*. **2017**, *7*, 2663.

(7) Jadapalli, J. K.; Wright, G. W.; Kain, V.; Sherwani, M. A.; Sonkar, R.; Yusuf, N.; Halade, G. V. Doxorubicin triggers splenic contraction and irreversible dysregulation of COX and LOX that alters the inflammation-resolution program in the myocardium. *Am. J. Physiol. Heart Circ. Physiol.* **2018**, *315*, H1091-H1100.

(8) Gorcsan III, J.; Tanaka, H. Echocardiographic Assessment of Myocardial Strain. *J. Am. Coll. Cardiol.* **2011**, *58*, 1401-1413.

(9) Lim, P.; Buakhamsri, A.; Popovic, Z. B.; Greenberg, N. L.; Patel, D.; Thomas, J. D.; Grimm, R. A. Longitudinal strain delay index by speckle tracking imaging: a new marker of response to cardiac resynchronization therapy. *Circulation* **2008**, *118*, 1130-1137.

(10) Tanaka, H.; Nesser, H. J.; Buck, T.; Oyenuga, O.; Janosi, R. A.; Winter, S.; Saba, S.; Gorscan III, J. Dyssynchrony by speckletracking echocardiography and response to cardiac resynchronization therapy: results of the Speckle Tracking and Resynchronization (STAR) study. *Eur. Heart J*. **2010**, *31*, 1690-1700.

(11)Tahover, E.; Patil, Y. P.; Gabizon, A. A. Emerging delivery systems to reduce doxorubicin cardiotoxicity and improve therapeutic index: focus on liposomes. *Anti-Cancer Drugs* **2015**, *26*, 241-258.

(12) Palazzolo, S.; Bayda, S.; Hadla, M.; Caligiuri, I.; Corona, G.; Toffoli, G.; Rizzolio, F. The Clinical Translation of Organic Nanomaterials for Cancer Therapy: A Focus on Polymeric Nanoparticles, Micelles, Liposomes and Exosomes. *Curr. Med. Chem*. **2018**, *25*, 4224-4268.

(13) Hu, H.; Liu, S.; Huang, Y.; Chen, X.; Jing, X. Biodegradable Block Copolymer-Doxorubicin Conjugates via Different Linkages: Preparation, Characterization, and In Vitro Evaluation. *Biomacromolecules* **2010**, *11*, 8, 2094-2102.

(14) Verma, A. K.; Leekha, A.; Kumar, V.; Moin, I.; Kumar, S. Biodistribution and In-vivo efficacy of doxorubicin loaded chitosan nanoparticles in Ehrlich Ascites Carcinoma (EAC) bearing Balb/C mice. *J. Nanomed. Nanotechnol*. **2018**, *9*, 1000510.

(15) Cao, A.; Ma, P.; Yang, T.; Lan, Y.; Yu, S.; Liu, L.; Sun, Y.; Liu, Y. Multifunctionalized Micelles Facilitate Intracellular Doxorubicin Delivery for Reversing Multidrug Resistance of Breast Cancer. *Mol. Pharmaceutics* 2019, DOI: 10.1021/acs.molpharmaceut.9b00094.

(16) Wang, J. Li, Y. Wang, L.; Wang, X.; Tu, P. Comparison of hyaluronic acid-based micelles and polyethylene glycol-based micelles on reversal of multidrug resistance and enhanced anticancer efficacy in vitro and in vivo. *Drug Delivery* **2018**, *25*, 330-340.

(17) Abebe, D. G.; Fujiwara, T. Controlled Thermo-Responsive Hydrogels by Stereocomplexed PLA-PEG-PLA Prepared via Hybrid Micelles of Pre-Mixed Copolymers with Different PEG Lengths. *Biomacromolecules*, **2012**, *13*, 1828-1836.

(18) Neuberger, T.; Schöpf, B.; Hofmann, H.; Hofmann, M.; von Rechenberg, B. Superparamagnetic Nanoparticles for Biomedical Applications: Possibilities and Limitations of a New Drug Delivery System. *J. Magnetism and Magnetic Mater*. **2005**, *293*, 483-496.

(19) Rose, T. A., Jr.; Choi, J. W. Intravenous Imaging Contrast Media Complications: The Basics That Every Clinician Needs to Know. *Am. J. Med*. **2015**, *128*, 943-949.

(20) Adair, J. H.; Parette, M. P.; Altınoglu, E. I.; Kester, M. Nanoparticulate Alternatives for Drug Delivery. *ACS Nano* **2010**, *4*, 4967-4970.

(21) Larson, N.; Ghandehari, H. Polymeric Conjugates for Drug Delivery. *Chem. Mater*. **2012**, *24*, 840-853.

(22) Messager, L.; Gaitzsch, J.; Chierico, L.; Battaglia, G. Novel Aspects of Encapsulation and Delivery Using Polymersomes. *Curr. Opin. Pharmacol*. **2014**, *18*, 104-111.

(23) Mohr, K.; Müller, S. S.; Müller, L. K.; Rusitzka, K.; Gietzen, S.; Frey, H.; Schmidt, M. Evaluation of Multifunctional Liposomes in Human Blood Serum by Light Scattering. *Langmuir* **2014**, *30*, 14954-14962.

(24) Lokerse, W. J. M.; Kneepkens, E. C. M.; ten Hagen, T. L. M.; Eggermont, A. M. M.; Grüll, H.; Koning, G. A. In Depth Study on Thermosensitive Liposomes: Optimizing Formulations for Tumor Specific Therapy and In Vitro to In Vivo Relations. *Biomaterials* **2016**, *82*, 138-150.

(25) Klibanov, A. L.; Maruyama, K.; Beckerleg, A. M.; Torchilin, V. P.; Huang, L. Activity of Amphipathic Poly(ethylene glycol) 5000 to Prolong the Circulation Time of Liposomes Depends on the Liposome Size and is Unfavorable for Immunoliposome Binding to Target. *Biochim. Biophys. Acta* **1991**, *1062*, 142-148.

(26) Needham, D.; Park, J.; Wright, A.; Tong, J. Materials Characterization of the Low Temperature Sensitive Liposome (ltsl): Effects of Lipid Composition (lysolipid and dspe-

peg2000) on the Thermal Transition and Release of Doxorubicin. *Faraday Discuss*. **2012**, 515-534.

(27) Contini, C.; Pearson, R.; Wang, L.; Messager, L.; Gaitzsch, J.; Rizzello, L.; Ruiz-Perez, L.; Battaglia, G. Bottom-Up Evolution of Vesicles from Disks to High-Genus Polymersomes. *iScience* **2018**, *7*, 132-144.

(28) Akimoto, J.; Nakayama, M.; Okano, T. Temperature-Responsive Polymeric Micelles for Optimizing Drug Targeting to Solid Tumors. *J. Control. Release* **2014**, *193*, 2-8.

(29) Lavasanifar, A.; Samuel, J.; Kwon, G. S. Poly(ethylene oxide)-block-Poly(L-amino acid) Micelles for Drug Delivery. *Adv. Drug Deliver. Rev*. **2002**, *54*, 169-190.

(30) Fang, J. S.; Gillies, R. D.; Gatenby, R. A. Adaptation to Hypoxia and Acidosis in Carcinogenesis and Tumor Progression. *Semin. Cancer Biol*. **2008**, *18*, 330-337.

(31) Tanner, P.; Baumann, P. ; Enea, R.; Onaca, O.; Palivan, C.; Meier, W. *Polymeric Vesicles: From Drug Carriers to Nanoreactors and Artificial Organelles. Acc. Chem. Res*. **2011**, *44*, 1039-1049.

(32) LoPresti, C.; Lomas, H.; Massignani, M.; Smart, T.; Battaglia, G. Polymersomes: Nature Inspired Nanometer Sized Compartments. *J. Mater. Chem*. **2009**, *19*, 3576-3590.

(33) Leong, J.; Teo, J. Y.; Aakalu, V. K.; Yang, Y. Y. Kong, H. Engineering Polymersomes for diagnostics and therapy. *Adv. Healthcare Mater*. **2018**, *7*, 1701276.

(34) Smith, A. E.; Xu, X.; Abell, T. U.; Kirkland, S. E.; Hensarling, R. M.; McCormick, C. L. Tuning Nanostructure Morphology and Gold Nanoparticle “Locking” of Multiply-Responsive Amphiphilic Diblock Copolymers. *Macromolecules* **2009**, *42*, 2958-2964.

(35) Flores, J. D.; Xu, X.; Treat. N. J.; McCormick, C. L. Reversible "Self-Locked" Micelles from a Zwitterion-Containing Triblock Copolymer. *Macromolecules* **2009**, 42, 4941-4945.

(36) Himanshu, A.; Sitasharan, P.; Singhai, A. K. Liposomes as Drug Carriers. *IJPLS* **2011**, *2*, 945-951.

(37) Zhou, Y.; Yan, D.; Dong, W.; Tian, Y. Temperature-Responsive Phase Transition of Polymer Vesicles: Real-Time Morphology Observation and Molecular Mechanism. *J. Phys. Chem. B* **2007**, *111*, 1262-1270.

(38) Li, M.-H.; Keller, P. Stimuli-Responsive Polymer Vesicles. *Soft Matter* **2009**, *5*, 927-937.

(39) Dan, M.; Huo, F.; Xiao, X.; Su, Y.; Zhang, W. Temperature-Sensitive Nanoparticle-to-Vesicle Transition of ABC Triblock Copolymer Corona-Shell-Core Nanoparticles Synthesized by Seeded Dispersion RAFT Polymerization. *Macromolecules* **2014**, *47*, 1360-1370.

(40) Marguet, M.; Edembe, L.; Lecommandoux, S. Polymersomes in Polymersomes: Multiple Loading and Permeability Control. *Angew. Chem*. **2012**, *124*, 1199-1202.

(41) Liao, J. F.; Wang, C.; Wang, Y. J.; Luo, F.; Qian, Z. Y. Recent Advances in Formation, Properties, and Applications of Polymersomes. *Curr. Pharm.Des*. **2012**, *18*, 3432-3441.

(42) Hu, X.; Zhang, Y.; Xie, Z.; Jing, X.; Bellotti, A.; Gu, Z. Stimuli-Responsive Polymersomes for Biomedical Applications. *Biomacromolecules* **2017**, *183*, 649-673.

(43) Kim, K. T.; Cornelissen, J. J.; Nolte, R. J.; Van Hest, J. C. A Polymersome Nanoreactor with Controllable Permeability Induced by Stimuli-Responsive Block Copolymers. *Adv. Mater*. **2009**, *21*, 2787-2791.

(44) Gebhardt, K. E.; Ahn, S.; Venkatachalam, G.; Savin, D. A. Role of Secondary Structure Changes on the Morphology of Polypeptide-Based Block Copolymer Vesicles. *J. Colloid Interface Sci.* **2008**, *317*, 70-76.

(45) Pearson, R. T.; Warren, N. J.; Lewis, A. L.; Armes, S. P.; Battaglia, G. Effect of pH and Temperature on PMPC-PDPA Copolymer Self-Assembly. *Macromolecules* **2013**, *46*, 1400-1407.

(46) Moquin, A.; Ji, J.; Neibert, K.; Winnik, F. M.; Maysinger, D. Encapsulation and Delivery of Neutrophic Proteins and Hydrophobic Agents Using PMOXA-PDMS-PMOXA Triblock Polymersomes. *ACS Omega* **2018**, *3*, 13882-13893.

(47) Wang, F.; Gao, J.; Xiao, J.; Du, J. Dually Gated Polymersomes for Gene Delivery. *Nano Lett*. **2018**, *18*, 5562-5568.

(48) Liang, X.; Kozlovskaya, V.; Cox, C. P.; Wang, Y. Saeed, M.; Kharlampieva, E. Synthesis and Self-Assembly of Thermosensitive Double-hydrophilic Poly(N-vinylcaprolactam)-b-poly(N-vinyl-2-pyrrolidone) Diblock Copolymers. *J. Polym. Sci. A: Polym. Chem*. **2014**, *52*, 2725-2737.

(49) Liang, X.; Liu, F.; Kozlovskaya, V.; Palchak, Z.; Kharlampieva, E. Thermoresponsive Micelles from Double LCST-Poly(3-methyl-N-vinylcaprolactam) Block Copolymers for Cancer Therapy. *ACS Macro Lett.* **2015**, *4*, 308-311

(50) Kubota, K.; Fujishige, S.; Ando, I. Single-Chain Transition of Poly(N-isopropylacrylamide) in Water. *J. Phys. Chem*. **1990**, *94*, 5154-5158.

(51) Maeda, Y.; Nakamura, T.; Ikeda, I. Hydration and Phase Behavior of Poly(N-vinylcaprolactam) and Poly(N-vinylpyrrolidone) in Water. *Macromolecules* **2002**, *35*, 217-222.

(52) Beija, M.; Marty, J.-D.; Destarac, M. Thermoresponsive poly(N-vinylcaprolactam)-Coated Gold Nanoparticles: Sharp Reversible Response and Easy Tunability. *Chem. Commun*. **2011**, 47, 2826-2828.

(53) Yu, Y. C.; Li, G.; Kim, J.; Youk, J. H. One-Pot Synthesis of Poly(N-vinylcaprolactam)-Based Biocompatible Block Copolymers using a Dual Initiator for ROP and RAFT Polymerization. *Polymer* **2013**, *54*, 6119-6124.

(54) Kermagoret, A.; Mathieu, K.; Thomassin, J-M.; Fustin, C-A.; Duchêne, R.; Jérôme, C.; Detrembleur, C.; Debuigne, A. Double Thermoresponsive Di- and Triblock Copolymers Based on N-vinylcaprolactam and N-vinylpyrrolidone: Synthesis and Comparative Study of Solution Behavior. *Polym. Chem*. **2014**, *5*, 6534-6544.

(55) Kozlovskaya, V.; Liu, F.; Xue, B.; Ahmad, F.; Alford, A.; Saeed, M.; Kharlampieva, E. Polyphenolic Polymersomes of Temperature-Sensitive Poly(N-vinylcaprolactam)-block-(poly(N-vinylpyrrolidone) for Anticancer Therapy. *Biomacromolecules* **2017**, *18*, 2552-2563.

(56) Kermagoret, A.; Fustin, C-A.; Bourguignon, M.; Detrembleur, C.; Jérôme, C.; Debuigne, A. One-Pot Controlled Synthesis of Double Thermoresponsive N-vinylcaprolactam-Based Copolymers with Tunable LCSTs. *Polym. Chem*. **2013**, *4*, 2575-2583.

(57) Wang, S-B.; Chen, A-Z.; Weng, L-J.; Chen, M-Y.; Xie, X-L. Effect of Drug-loading Methods on Drug Load, Encapsulation Efficiency and Release Properties of Alginate/Poly-L-Arginine/Chitosan Ternary Complex Microcapsules. *Macromol. Biosci*. **2004**, *4*, 2-30.

(58) Heller, W.T.; Cuneo, M.J.; Debeer-Schmitt, L.M.; Do, C.; He, L.; Heroux, L.; Littrell, K.C.; Pingali, S.V.; Qian, S.; Stanley, C.B.; Urban, V.S.; Wu, B.; Bras, W. The Suite of Small-angle

neutron Scattering Instruments at Oak Ridge National Laboratory", *J. App. Cryst.* 2018, *51*, 242-248.

(59) Kline, S. R. Reduction and Analysis of SANS and USANS Data using IGOR Pro. *J. Appl. Crystallogr.* **2006**, *39*, 895-900.

(60) Kim, M. D.; Dergunov, S. A.; Richter, A. G.; Durbin, J.; Shmakov, S. N.; Jia, Y.; Kenbeilova, S.; Orazbekuly, Y.; Kengpeiil, A.; Lindner, E.; Pingali, S. V.; Urban, V.S.; Weigand, S.; Pinkhassik, E. Facile Directed Assembly of Hollow Polymer Nanocapsules within Spontaneously Formed Catanionic Surfactant Vesicles. *Langmuir* **2014**, *30*, 7061−7069.

(61) Richter, A. G.; Dergunov, S.A.; Ganus, B.; Thomas, Z.; Pingali, S. V.; Urban, V.; Liu, Y.; Porcar, L.; Pinkhassik, E. Scattering Studies of Hydrophobic Monomers in Liposomal Bilayers: An Expanding Shell Model of Monomer Distribution. *Langmuir* **2011**, *27*, 3792–3797.

(62) Hammouda, B. A New Guinier-Porod Model. *J. Appl. Cryst.* **2010**, *43*, 716-719.

(63) Jadapalli, J. K.; Wright, G. W.; Kain, V.; Sherwani, M. A.; Sonkar, R.; Yusuf, N.; Halade. G. V. Doxorubicin Triggers Splenic Contraction and Irreversible Dysregulation of COX and LOX that Alters the Inflammation-Resolution Program in the Myocardium. *Am. J. Physiol. Heart .Circ. Physiol.* **2018**, *315*, H1091-H1100.

(64) Chen, G.-T.; Wang, C.-H.; Zhang, J.-G.; Wang, Y.; Zhang, R.; Du, F.-S.; Yan, N.; Kou, Y.; Li, Z.-C. Toward Functionalization of Thermoresponsive Poly(N-vinyl-2-pyrrolidone). *Macromolecules* **2010**, *43*, 9972-9981.

(65) Liu, F.; Kozlovskaya, V.; Medipelli, S.; Xue, B.; Ahmad, F.; Saeed, M.; Cropek, D.; Kharlampieva, E. Temperature-Sensitive Polymersomes for Controlled Delivery of Anticancer Drugs. *Chem. Mater*. **2015**, *27*, 7945-7956.

(66) Jennings, J.; Beija, M.; Kennon, J. T.; Willcock, H.; O'Reilly, R. K.; Rimmer, S.; Howdle, S. M. Advantages of Block Copolymer Synthesis by RAFT-Controlled Dispersion Polymerization in Supercritical Carbon Dioxide. *Macromolecules* 2013, 46, 6843-6851.

(67) Chuangchote, S.; Sagawa, T.; Yoshikawa, S. Electrospinning of Poly(vinyl pyrrolidone): Effects of Solvents on Electrospinnability for the Fabrication of Poly(p-phenylene vinylene) and TiO_2 Nanofibers. *J. Applied Polym. Sci*. **2009**, **114**, 2777-2791.

(68) Wilczek-Vera, G.; Danis, P. O.; Eisenberg, A. Individual Block Length Distributions of Block Copolymers of Polystyrene-block-Poly(R-methylstyrene) by MALDI/TOF Mass Spectrometry. *Macromolecules* **1996**, *29*, 4036-4044.

(69) Liu, J.; Debuigne, A.; Detrembleur, C.; Jérôme, C. Poly(N-vinylcaprolactam): a thermoresponsive macromolecule with promising future in biomedical field. *Adv. Healthc. Mater*. **2014**, *3*, 1941-1968.

(70) Tang, S.; Cao, Y.; Goddard, S. C.; He, W. Synthesis of 3-(tert-Butoxycarbonylmethyl)-N-vinyl-2-caprolactam and Homologous Copolymerization Toward Biocompatible Carboxylated Poly (N-vinyl-2-caprolactam) Responsive to pH and Temperature. *J. Polym. Sci. Part A: Polym. Chem*. **2014**, *52*, 112-120.

(71) Zhang, J.; Yuan, Y.; Kilpin, K. J. Kou, Y.; Dyson, P. J.; Yan, N. Thermally responsive gold nanocatalysts based on a modified polyvinylpyrrolidone. *J. Mol. Catal. A Chem*. **2013**, *371*, 29-35.

(72) Zhao, X.; Coutelier, O.; Nguyen, H. H. Delmas, C.; Destarac, M.; Marty, J. D. Effect of Copolymer Composition of RAFT/MADIX-Derived N-vinylcaprolactam/N-vinylpyrrolidone Statistical Copolymers on Their Thermoresponsive Behavior and Hydrogel Properties. *Polym. Chem*. **2015**, *6*, 5233-5243.

(73) Yang, Y.; Alford, A.; Kozlovskaya, V.; Zhao, S.; Joshi, H.; Kim, E.; Qian, S.; Urban, V.; Cropek, D.; Aksimentiev, A.; Kharlampieva, E. Effect of Temperature ad Hydrophilic Ratio on the Structure of Poly(N-vinylcaprolactam)-block-poly(dimethylsiloxane)-block-poly(N-vinylcaprolactam) Polymersomes. *ACS Applied Polym. Mater*. **2019**, *1*, 722-736.

(74) Danafar, H.; Rostamizadeh, K.; Davaran, S.; Hamidi, M. PLA-PEG-PLA Copolymer-Based Polymersomes as Nanocarriers for Delivery of Hydrophilic and Hydrophobic Drugs: Preparation and Evaluation with Atorvastatin and Lisinopril. *Drug Dev. Ind. Pharm*. **2014**, *40*, 1411-1420.

(75) Lee, J. S.; Feijen, J. Polymersomes for Drug Delivery: Design, Formation and Characterization. *J. Control. Release* **2012**, *161*, 473-483.

(76) Pawar, P. V.; Gohil, S. V.; Jain, J. P.; Kumar, N. Functionalized polymersomes for biomedical applications. *Polym. Chem*. **2013**, *4*, 3160-3176.

(77) Xu, J.; Zhao, Q.; Jin, Y.; Qiu, L. High Loading of Hydrophilic/Hydrophobic Doxorubicin into Polyphosphazene Polymersome for Breast Cancer Therapy. *Nanomedicine* **2014**, *10*, 349-358.

(78) Oliveira, H.; Pérez-Andrés, E.; Thevenot, J.; Sandre, O.; Berra, E.; Lecommandoux, S. Magnetic field triggered drug release from polymersomes for cancer therapeutics. *J. Control. Release* **2013**, *169*, 165-170.

(79) Gasselhuber, A.; Dreher, M. R.; Negussie, A.; Wood, B. J.; Rattay, F.; Haemmerich, D.; Mathematical Spatio-Temporal Model of Drug Delivery from Low Temperature Sensitive Liposomes During Radiofrequency Tumour Ablation. *Int. J. Hyperth*. **2010**, *26*, 499-513.

(80) Li, L.; ten Hagen, T. L. M.; Hossann, M.; Süss, R.; van Rhoon, G. C.; Eggermont, A. M. M.; Haemmerich, D.; Koning, G. A. Mild hyperthermia triggered doxorubicin release from optimized stealth thermosensitive liposomes improves intratumoral drug delivery and efficacy. *J. Control. Release* **2013**, *168*, 142-150.

(81) Andersen, T. E.; Palarasah, Y.; Skjødt, M. O.; Ogaki, R.; Benter, M.; Alei, M.; Kolmos, H. J.; Koch, C.; Kingshott, P. Decreased Material-Activation of the Complement System Using Low-Energy Plasma Polymerized Poly(vinyl pyrrolidone) Coatings. *Biomaterials* **2011**, *32*, 4481-4488.

(82) Gaucher, G.; Asahina, A.; Wang, J.; Leroux, J. C. Effect of Poly(N-vinyl-pyrrolidone)-block-poly(d,l-lactide) as Coating Agent on the Opsonization, Phagocytosis, and Pharmacokinetics of Biodegradable Nanoparticles. *Biomacromolecules* **2009**, *10*, 408-416.

(83) Lasic, D. D.; Needham, D. The "Sealth" Liposome: A Prototypical Biomaterial. *Chem. Rev*. **1995**, *95*, 2601-2628.

(84) Rösler, A.; Vandermeulen, G. W.; Klok, H. A. Advanced Drug Delivery Devices via Self-Assembly of Amphiphilic Block Copolymers. *Adv. Drug Deliv. Rev*. **2012**, *64*, 270-279.

(85) Chen, J.; Ratnayaka, S.; Alford, A.; Kozlovskaya, V.; Liu, F.; Xue, B.; Hoyt, K.; Kharlampieva, E. Theranostic Multilayer Capsules for Ultrasound Imaging and Guided Drug Delivery. *ACS Nano* **2017**, *11*, 3135-3146.

(86) Alford, A.; Rich, M.; Kozlovskaya, V.; Chen, J.; Sherwood, J.; Bolding, M.; Warram, J.; Bao, Y.; Kharlampieva, E. Ultrasound-Triggered Delivery of Anticancer Therapuetics from MRI-Visible Multilayer Microcapsules. *Adv. Therapeutics* **2018**, *1*, 1800051.

(87) Shi, L.; Chapman, T. M.; Beckman, E. J. Poly(ethyleneglycol)-block-poly(N-vinylformamide) Copolymers Synthesized by the RAFT Methodology. *Macromolecules* **2003**, *36*, 2563-2567.

(88) Keddie, D. J.; Moad, G.; Rizzardo, E.; Thang, S. H. RAFT Agent Design and Synthesis. *Macromolecules* **2012**, *45*, 5321-5342.
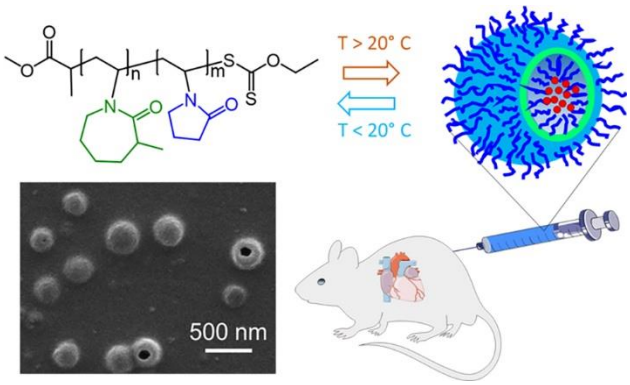
Table of Contents graphic